Journal of Applied Sciences

ISSN 1812-5654

science alert

ANSInet
an open access publisher
http://ansinet.com

Journal of Applied Sciences 7 (6): 903-912, 2007
ISSN 1812-5654

External Horizontally Uniform Magnetic Field Applied to Steel Solidification

[1]Farid Mechighel and [2]Mahfoud Kadja
[1]Laboratoire de Mécanique Industrielle, Department of Mechanical Engineering,
Annaba University, Annaba, Algeria
[2]Laboratoire d'énergétique Appliquée et de Pollution, Department of Mechanical Engineering,
Constantine University, Constantine, Algeria

Abstract: Based on continuum model, a mathematical model for convection flow during directional solidification of steel, Fe-0.42wt%C, in an applied magnetic field is presented. The model includes mass, momentum, energy, species and electrical potential conservation equations. The geometry under study is rectangular. The permeability in the mushy zone is treated by means of the Blake-Kozeny equation. The system of equation has been discretized by means of Finite volume method. For solution of discretized equations SIMPLER Algorithm is used. The results show the strong effect of the magnetic field on the solidification process.

Key words: Thermo-solutal convection, magnetic field, eutectic solidification, electromagnetic convection

INTRODUCTION

In recent years, numerical simulations have shown the ability of macroscopic solidification models to predict the effects of convection in the mushy zone and bulk liquid on the development of an irregular liquidus front, flow channels in the mushy zone, local remelting of solid and complicated macrosegregation for the solidification of a variety of binary alloys. The cause of macrosegregation is the long-range advection of alloy species due to the relative movement or flow of segregated liquid and solid during solidification. There are numerous causes of fluid flow and solid movement in casting processes: flow that feeds the solidification shrinkage and the contractions of the liquid and solid during solidification; buoyancy forces induced thermo-solutal convection flows due to thermal and solutal gradients in the liquid; these forces can either aid or oppose each other, depending on the direction of the thermal gradient and whether the rejected solutes cause an increase or a decrease in the density of the liquid; forced flows due to: applied magnetic fields, stirring, rotation, vibration, etc., (Beckermann, 2002). Therefore, the need to prevent macrosegregation during solidification processing is extremely important.

To prevent macrosegregation all efforts are aimed at controlling fluid flow and solid movement for example: include adjustments to the alloy composition or thermal gradients to induce a stable density stratification in the liquid; include centrifugal forces, or electromagnetic fields to redistribute the flow (Beckermann, 2002).

Macrosegregation is an important defect in steel casting and there have been few macrosegregation studies, where no external magnetic is applied, on iron-carbon and iron-carbon based steel. Ma *et al.* (2004) have performed a numerical simulation of macro-segregation in Fe-0.42wt%C steel ingot during solidification. Liu (2004) has presented numerical modeling for the macrosegregation in the Fe-0.2wt%C steel. Also, Singh and Basu (2001a, 2001b) have presented simulations to study the role of double diffusive convection on macrosegregation during solidification of binary Fe-1wt%C alloy, where, The effect of thermo-solutal convection on extent of macrosegregation profile is discussed.

The modeling of the formation of macrosegregation in steel due to multi-component thermo-solutal convection was explored in detail by Schneider and Beckermann (1995a), where, by using a fully coupled multi-component model, they have shown that macrosegregation profiles of carbon in multi-component steel show the same trend as in binary Fe-C owing to dominant role of carbon in solutal buoyancy and thermodynamic equilibrium. Another work performed, by Schneider and Beckermann (1995b), for study of solidification, where no external magnetic is applied, the simulation of the austenitic solidification steels containing ten elements in a rectangular cavity cooled from the side shows the formation of macrosegregation, channel segregates and islands of mush surrounded by the bulk melt. The global severity of macrosegregation of an element is found to be linearly dependent on its partition coefficient.

Corresponding Author: Farid Mechighel, Laboratoire de Mécanique Industrielle, Department of Mechanical Engineering, Annaba University, Annaba, Algeria Tel: 00213-6367-3272 Fax: 00213-3720-6566

Moreover, several studies have been carried out where a magnetic field is applied during solidification for different binary alloys. We note here the study due to Sampath and Zabaras (2001), where the system Sb-Ge is considered for study of the thermo-solutal and capillary convection. Also, the study carried out by Anwar Hossain *et al.* (2005) and the study performed by Mittal *et al.* (2005).

In the present study the influence of an external magnetic field, applied during solidification process of the system Fe-0.42wt%C, on the flows control, especially the control of the advection of solute in the liquid phase near the front of solidification (solutal convection flow the main cause of macrosegregation).

MATHEMATICAL MODEL

Consider a mold permeated by a uniform magnetic field B of constant magnitude B_0 in the axial direction, shown on Fig. 1. The mold is of rectangular geometry with length and height L = 60 mm. This mold, of impermeable to all species walls and no-slip velocity conditions were imposed at the walls, contained a molten electrically conducting binary alloy Iron-carbon (Fe-0.42wt%C), of a eutectic temperature (T_e = 1147°C). The thermo-physical properties of this alloy (Ma *et al.*, 2004) are listed in Table 1. All thermo-physical properties are assumed constant. The molten alloy was initially isothermal, at a uniform concentration C_{ini}= 0.42% and a uniform temperature T_{ini} = 1528°C.

At time t = 0, the left wall is suddenly cooled to a temperature T_{cold} = 1100°C and maintained at that temperature for times t > 0. The other right, top and bottom walls are insulated and adiabatic. The temperature at the right wall is imposed to be T_{hot} = 1528°C. Under these conditions the directional solidification begins. The motion of the melt is initially driven by the action of the combined of thermal-solutal buoyancy forces and a Lorentz force.

Electromagnetic lorentz force: The concentration of the solute in the liquid phase near the front of solidification must be controlled to ensure the control of macrosegregation which improve the homogeneity and the quality of the solid formed. The control is possible by the application of an external uniform magnetic field in order to suppress fluctuations due to density irregularities provoked by concentration gradients.

Lorentz force F of component (Fx, Fy) drives electromagnetic convection flow is given, in such flow, as follows:

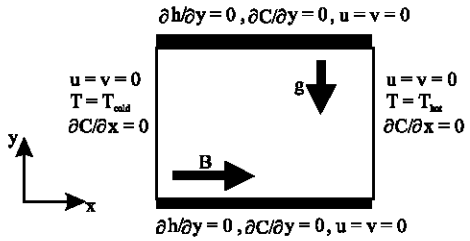

Fig. 1: Mold geometry

Table 1: Thermo-physical properties for Fe-0.42wt%C system, (Ma *et al.*, 2004)

Melting point [from diagram]	T_f (°C)	1535
Latent heat	L_H (J kg^{-1})	2.7132×10^{5}
Density of the melt	ρ_l (kg m^{-3})	7300
Thermal expansion coefficient	β_T (1 K^{-1})	2.0×10^{-4}
Solutal expansion coefficient	β_S (1/wt%)	1.10
Viscosity of the melt	μ_l (kg ms^{-1})	6.0×10^{-4}
Solute liquid diffusivity	D_l (m^2 s^{-1})	4.8×10^{-9}
Specific heat of melt	cp_l (J kg^{-1})	726.6
Thermal conductivity of the melt	k_l (W/m K)	28.56
Electrical conductivity for solid and melt [assumed from physics handbooks]	σ_e (S/m)	5.88×10^{6}
Liquidus slope [calculated from diagram]	m (K/wt%)	-9201.03
Partition coefficient	K_P	0.30
Permeability coefficient	K_0 (m^2)	5.56×10^{-11}

$$F = q_e E + J \times B \quad (1)$$

where: q_e is the electric charge density of the fluid.

And the electric field intensity E, given in term of the electric field potential φ,

$$E = -\nabla\varphi \quad (2)$$

And, J the electric current density that is governed by Ohm's law:

$$J = \sigma_e (-\nabla\varphi + V \times B) \quad (3)$$

where: V is the velocity vector of flow field.

In addition to Ohm's law, the electric current density J is governed by the conservation of electric current that is given, for a moving medium, as:

$$\nabla \bullet J = 0 \quad (4)$$

In addition to the applied magnetic field B of constant intensity B_0, there is an induced magnetic field produced by the electric currents in the liquid metal. Since, it is assumed that the walls of the cavity are electric insulators and the magnetic Reynolds number is sufficiently small such that the induced magnetic field is negligible with respect to the imposed constant magnetic field B_0, therefore neglecting excess charge i.e.,:

$$(F \approx J \times B) \quad (5)$$

The mold is with electrically insulated boundaries in the present of two-dimensional flow the electric potential φ is constant, (Anwar Hossain *et al*., 2005), therefore:

$$\nabla\varphi = 0 \quad (6)$$

Assumptions:

- We assume that the solidus line, in the Fe-C binary equilibrium diagram, as linear.
- As we know the solid phases which can be occur in Fe-0.42wt%C steel solidification are the following: the primary solid phase: γ(Austenitic), the secondary solid phase: Fe_3C(Comentite) and the eutectic component: γ(Austenitic) + Fe_3C(Comentite) resulted from the eutectic reaction. Therefore, we assume that only the following eutectic reaction, of solidification, occurs in the molten alloy. Therefore, no peritectic reaction is assumed:

$$\text{Liquid}(\text{Fe}-0.42\text{C}) \Rightarrow \gamma(\text{Austenitic}) + \text{Fe}_3\text{C}(\text{Cementite})$$

- Assuming that, these solid phases can be presented by a single solid phase. Because the present study does not interest to the different solid phases analyze.

Also considering the following assumptions:

- Two-phase flows are described as a mixture of solid and liquid phases,
- Local thermodynamic equilibrium exists between solid and liquid phases (therefore, the phase diagram is used and the formulation due to Bennon and Incropera (1987) will be used).
- All of the properties of the mixture can be obtained from each phase component properties. All transport properties are constant.
- The mushy region, (austenite+ liquid) interface is modeled by means of isotropic permeability approach, using equation of Blake-Kozeny.
- It has no Joule heating effects.
- The intrinsic velocity of the solid phase is neglected.
- The flow of the liquid phase is assumed to be laminar.
- Densities in the solid and liquid are constant except for the variations in the buoyancy term (we consider the Boussinesq approximation).

Governing equations: Based on continuum model, (Bennon and Incropera, 1987), governing equations for binary alloy solidification are represented by: the mass, momentum, energy, species and electrical potential conservation equations (7 to 12), as reported by Ma *et al*. (2004) except here we add the Lorentz force term in the y-direction momentum equation and we have the conservation of electrical potential equation.

These equations can be written in dimension less form, respectively, (Mechighel and Kadja, 2006). In this dimension less form: we defining characteristic scales for: length, velocity, time, temperature, enthalpy, species concentration and electric potential, respectively as following:

$$x_c = L,\ U_c = \sqrt{g\beta_T \Delta T\, L},\ t_c = \sqrt{L/g\beta_T \Delta T},$$
$$\Delta T = T_{liq} - T_{ref},\ cp_l \Delta T,\ \Delta C = m^{ad}\Delta T/m \text{ and } v_l B_0$$

where: m^{ad} is the dimension less slope of the liquidus line, T_{liq}: is the liquidus temperature and T_{ref}: is the reference temperature.

Therefore, the dimension less coordinates, the dimension less mixture velocity components, the dimension less continuum mixture enthalpy the dimension less continuum mixture composition and the dimension less electrical potential are given, respectively, as following:

$$X = x/L,\quad Y = y/L,\quad U = u/U_c,\quad V = v/U_c,$$
$$H = (h - h_{ref})/cp_l\Delta T,\ X = (C - C_{ref})/\Delta C \text{ and } \Phi = \varphi/v_l B_0$$

where: (x, y): the Cartesian coordinates, (u, v): the velocity components, h: the enthalpy and C: the concentration.

Also, the dimension less temperature is given such as:

$$\Theta = (T - T_{ref})/\Delta T$$

In Table 2 are listed the resulting dimension less numbers:

$$Da = K_0/L^2,\ Pr = v_l/\alpha_l,\ Gr = g\beta_T \Delta T L^3/v_l^2,\ Sc = v_l/D_l,$$
$$Ha = B_0 L\sqrt{\sigma_e/\rho_l v_l} \text{ and } Ste = L_H/Cp_l\Delta T$$

where: α_l the melt thermal diffusivity, v_l the melt kinematical viscosity and g: acceleration of gravity.

The other dimension less parameters include, respectively, the specific heat ratio, the heat conductivity ratio and buoyancy ratio:

$$CP = cp_s/cp_l,\ Rk = k_s/k_l \text{ and } N = \beta_s\Delta C/\beta_T\Delta T$$

In the case where the magnetic field is applied horizontally, therefore:

Table 2: Calculated dimension less numbers using data given by Ma *et al.* (2004) and other parameters for Fe-0.42wt%C

Darcy number	Da	154.44×10^{-10}
Prandtl number	Pr	0.01526
Grashof number	Gr	22.39567×10^{8}
Schmidt number	Sc	17.12
Hartmann number	Ha (B_0=0.05 Tesla)	$5940.86\,B_0$
Stefan number	Ste	1.045
Specific heat ratio	CP	1.0
Heat conductivity ratio	Rk	1.0
Buoyancy ratio	N	0.597759

$$F_x = 0 \text{ and } F_y = -\frac{Ha^2}{Gr^{0.5}}\left[(\sigma_e V)\right]$$

The governing equations, in dimension less form are:

$$\frac{\partial \rho}{\partial t} + \nabla\cdot\left(\rho\vec{V}\right) = 0 \tag{7}$$

$$\frac{\partial(\rho U)}{\partial t} + \nabla\cdot\left(\rho\vec{V}U\right) = -\frac{\partial P}{\partial x} + \frac{1}{Gr^{0.5}}\nabla\cdot(\rho\nabla U) - \frac{1}{Da\,Gr^{0.5}}\frac{(1-\varepsilon_l)^2}{\varepsilon_l^3}\rho U \tag{8}$$

$$\frac{\partial(\rho V)}{\partial t} + \nabla\cdot\left(\rho\vec{V}V\right) = -\frac{\partial p}{\partial y} + \frac{1}{Gr^{0.5}}\nabla\cdot(\rho\nabla V) - \frac{1}{Da\,Gr^{0.5}}\frac{(1-\varepsilon_l)^2}{\varepsilon_l^3}\rho V + (\Theta + NX_l) - \frac{Ha^2}{Gr^{0.5}}\left[(\sigma_e V)\right] \tag{9}$$

$$\frac{\partial(\rho H)}{\partial t} + \nabla\cdot\left(\rho\vec{V}H\right) = \frac{1}{PrGr^{\frac{1}{2}}}\nabla\cdot\left(\frac{1+\varepsilon_s(Rk-1)}{CP}\nabla H\right) + \frac{1}{PrGr^{\frac{1}{2}}}\nabla\cdot\left(\frac{1+\varepsilon_s(Rk-1)}{CP}\nabla(H_l - H)\right) - \nabla\cdot\left[f_l\rho\vec{V}(H_l - H_s)\right] \tag{10}$$

$$\frac{\partial(\rho X)}{\partial t} + \nabla\cdot\left(\rho\vec{V}X\right) = \frac{1}{Sc\,Gr^{\frac{1}{2}}}\nabla\cdot\left((1-f_s)\rho\nabla X\right) + \frac{1}{ScGr^{\frac{1}{2}}}\nabla\cdot\left((1-f_s)\rho\nabla(X_l - X)\right) - \nabla\cdot\left[f_s\rho\vec{V}(X_l - X_s)\right] \tag{11}$$

$$\nabla^2\Phi = 0 \tag{12}$$

where:

ρ : Is the mixture dimensionless density
f_s : Is the solid mass fraction
$(\varepsilon_l, \varepsilon_s)$: Are the melt and solid volume fractions, respectively.

While, the subscripts:

s : Used to identify the solid phase
l : Used to identify the liquid phase

Isotropic model for mushy: The Blake-Kozeny equation for calculated the permeability in the mushy zone is given by:

$$K = K_0\,\varepsilon_l^3/(1-\varepsilon_l)^2 \tag{13}$$

K_0 is a parameter depending on the morphology and size of the primary dendrite arm spacing: λ_1.

The parameter K_0 is given by Singh and Basu (2001a), such as:

$$K_0 = \frac{\lambda_1^2}{180}$$

Thermodynamic equilibrium: Since it is assumed that the local thermodynamic equilibrium exists between the solid and liquid phases, thermo-physical properties of each phase are constant (but different from each other) and the liquidus and solidus lines on the equilibrium phase diagram are linear. Hence, the supplementary relations of Bennon and Incropera (1987) can be used.

With the full coupling, in the mushy zone, of the temperature field and species concentration through thermodynamic equilibrium requirements Temperature and concentration is represented through the following equation:

$$T = T_f + mC \tag{14}$$

Also, the temperature and solid mass fraction will be calculated from the continuum enthalpy and concentration. Therefore, phase diagram will be used. In addition, local solid and liquid densities are determined and boundary enthalpies are appropriately adjusted.

NUMERICAL SOLUTION

The system of the governing equations, with the coupling of the temperature and concentrations and the coupling of temperature and mass fraction solid, has been discretized by means of volume based finite difference method (Patankar, 1980). For the resolution of discretized

equations obtained the SIMPLER Algorithm is used, (Patankar, 1980). And for the resolution of the algebraically system equations obtained the Thomas Algorithm is used.

The selected mesh size should only be viewed as a compromise between accuracy and computational cost associated with such simulations. A mesh of 50*50 nodes in the domain and a constant dimensionless time step of $\Delta t = 0.005$ were used.

RESULTS AND DISCUSSION

Results presented by Ma *et al.* (2004) for the solidification of the binary system Fe-0.42wt%C, results presented by Liu (2004) for the solidification of the binary system Fe-0.2wt%C and results carried out by Singh and Basu (2001a and b) for the solidification of the binary system Fe-1wt%C, where no magnetic field is applied, shown the large effect of the convective flow driven by thermal-solutal buoyancy forces on the solidifying product: large values of velocities, macrosegreagation and other defects.

For our case we applied a magnetic field for controlling convection flow.

Early stage of solidification: For the convective flow field, under an external magnetic field, streamlines, liquid isocompositions, isotherms, solid mass fraction and solutes distribution field corresponding to the early stage of the solidification process, at t = 10, are presented in Fig. 2a-e, respectively.

Convection flow field: Figure 2a shows the coupled effects of electromagnetic and buoyancy driven convection reversal flow.

One can see that horizontal gradients of temperature and solute concentration in the liquid are built up at this early stage of solidification. These two gradients lead to a horizontal gradient of the liquid density. Hence, thermal and solutal forces driven natural convection coupled with Lorentz force driven forced convection (electromagnetically convection) occur in the mold.

For the Fe-0.42wt%C alloy, the interdendritic liquid, in the mushy zone, is enriched in solute (Carbon), Fig. 2b, becomes lighter (since the density of Carbon is lower than that of Iron), the effects of solute concentration and temperature on the liquid density are opposite, but solute-induced convection dominates in the mushy zone, leading a clockwise fluid flow but this flow is extremely weak. This is due to fact that the buoyancy ratio is too small N = 0.59.

The thermal buoyancy force is dominant the melt flow this is due to the fact that the liquid is superheated at the beginning of the solidification and the low value of solutal buoyancy force in the liquid. Therefore, the solutal opposes the thermal buoyancy forces, in the mushy. While, the Lorentz force acts in opposition to the thermal buoyancy force on the liquid flow, Eq. 9. Therefore, the application of the externally magnetic field reduces the velocity vectors and leads to damping out turbulence and intensity of melt flow, thereby improving the homogeneity of the solid formed.

The reversal flow observed in the melt region, Fig. 2a, is a typical feature of natural convection coupled with forced convection in a stratified fluid, (Sampath and Zabaras, 2001; Sampath, 2001).

Solute concentration and temperature fields: Isotherms, in Fig. 2c, are nearly vertical, indicating one-dimensional horizontal conduction in solid formed.

In Fig. 2b and e, one can see 2 levels where the solutes are rejected in the mushy zone, the first level is at approximately Y = 0.95 and the second, extremely important, is near the bottom of the mold.

The rejected solutes lead to a complicated interface form, Fig. 2b. This is due essentially to the system chosen in this study, characterized by a large Lewis number (Le = Sc/Pr = 1122), for this system the solutal mushy boundary layer is extremely thin and concentration gradients are very high close to the interface, which lead to an increase of the rejected solutes in the mushy. The fluid in the mushy, have an increasing composition, from the nominal value ($X_0 = 0.108$) towards to the value (X = 0.36) but not be eutectic (Xe = 1.108), Fig. 2b. While, the temperature is decreasing from the value (1.06) towards the eutectic value (0.0), Fig. 2c.

In Fig. 2e, the dominant thermally buoyancy forces drive downward the solutes rejected from the mushy zone for to be re-melting in the bulk melt. Likewise, one can see that the Carbon begins to accumulate at the bottom while the Iron begins to accumulate at the top of the mold.

Solid mass fraction: Figure 2d shows the solid fraction formed for this stage of solidification. The bulk mass fraction of the solid formed; Fig. 2d; need not be eutectic because of the presence of the thin thickness mushy layer and is instead controlled by mass transfer within the fluid.

Intermediate stage of solidification: For the convective flow field, under an external magnetic field, streamlines, liquid isocompositions, isotherms, solid mass fraction and solutes distribution field corresponding to the intermediate stage of the solidification process, at t = 150, are presented in Fig. 3a-e, respectively.

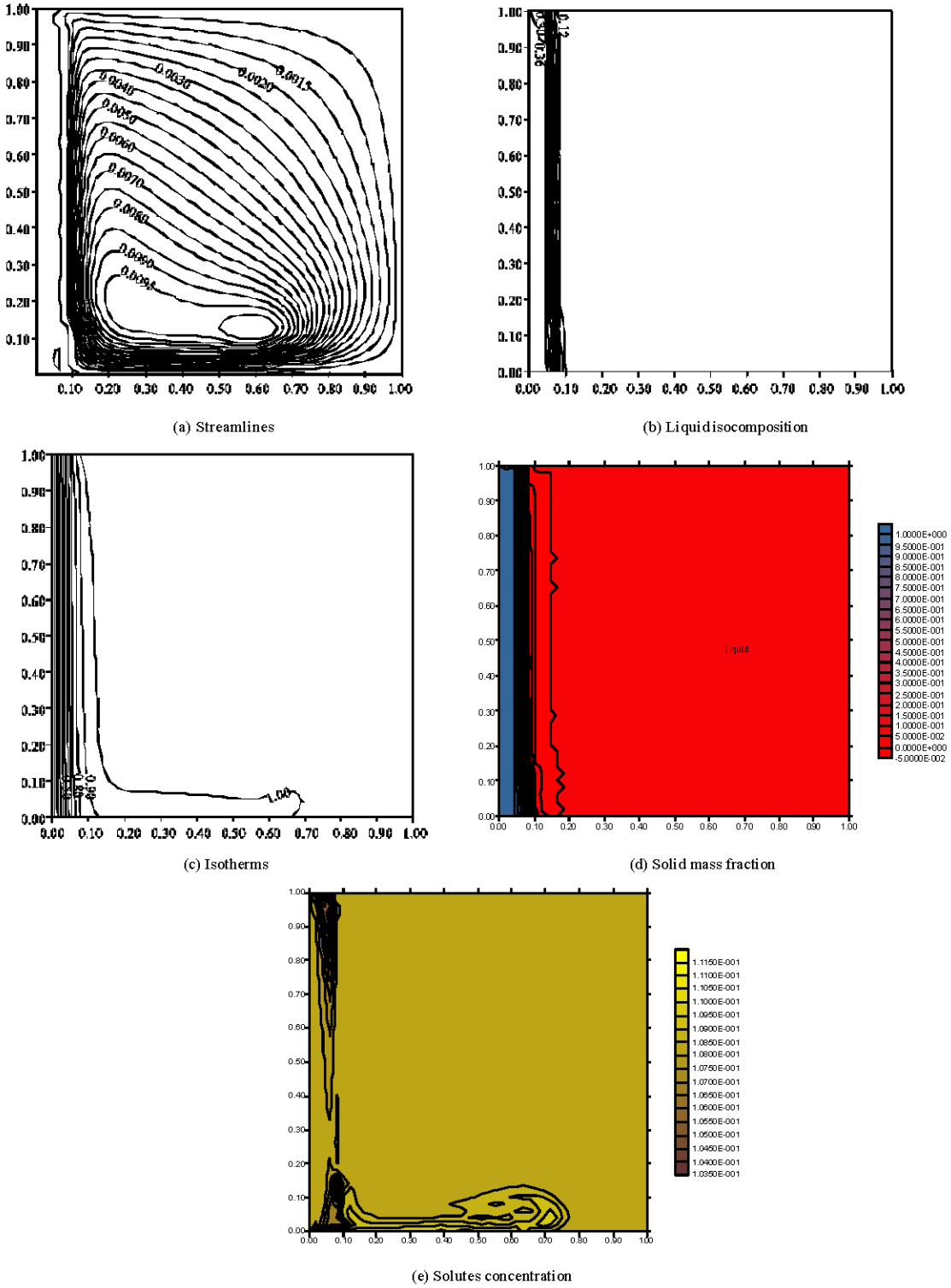

Fig. 2: Solidification at time = 10, (a) Streamlines, (b) Liquid isocomposition (c) Isotherms, (d) Solid mass fraction and (e) Solutes concentration

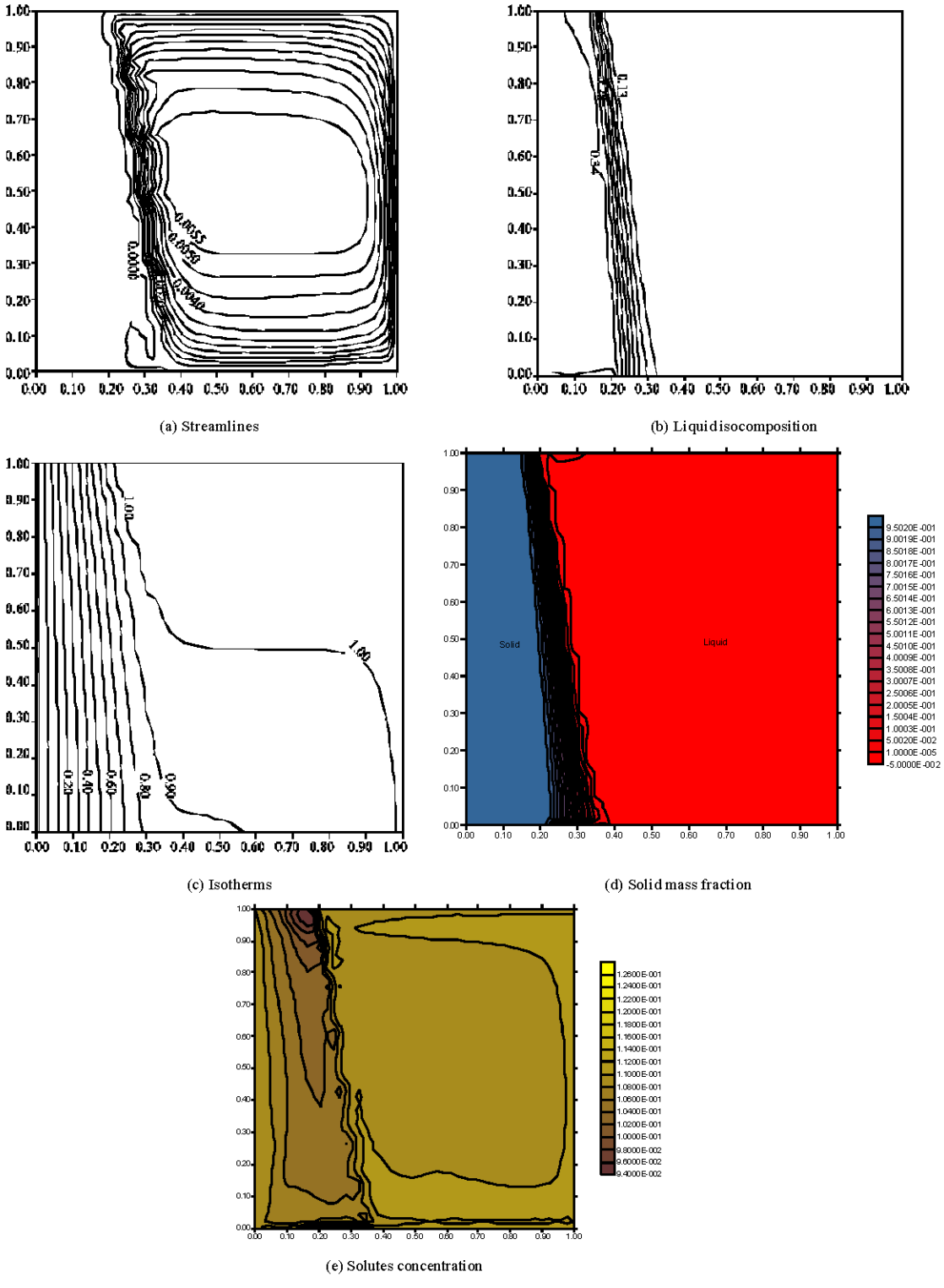

Fig. 3: Solidification at time = 150, (a) Streamlines, (b) Liquid isocomposition (c) Isotherms, (d) Solid mass fraction and (e) Solutes concentration

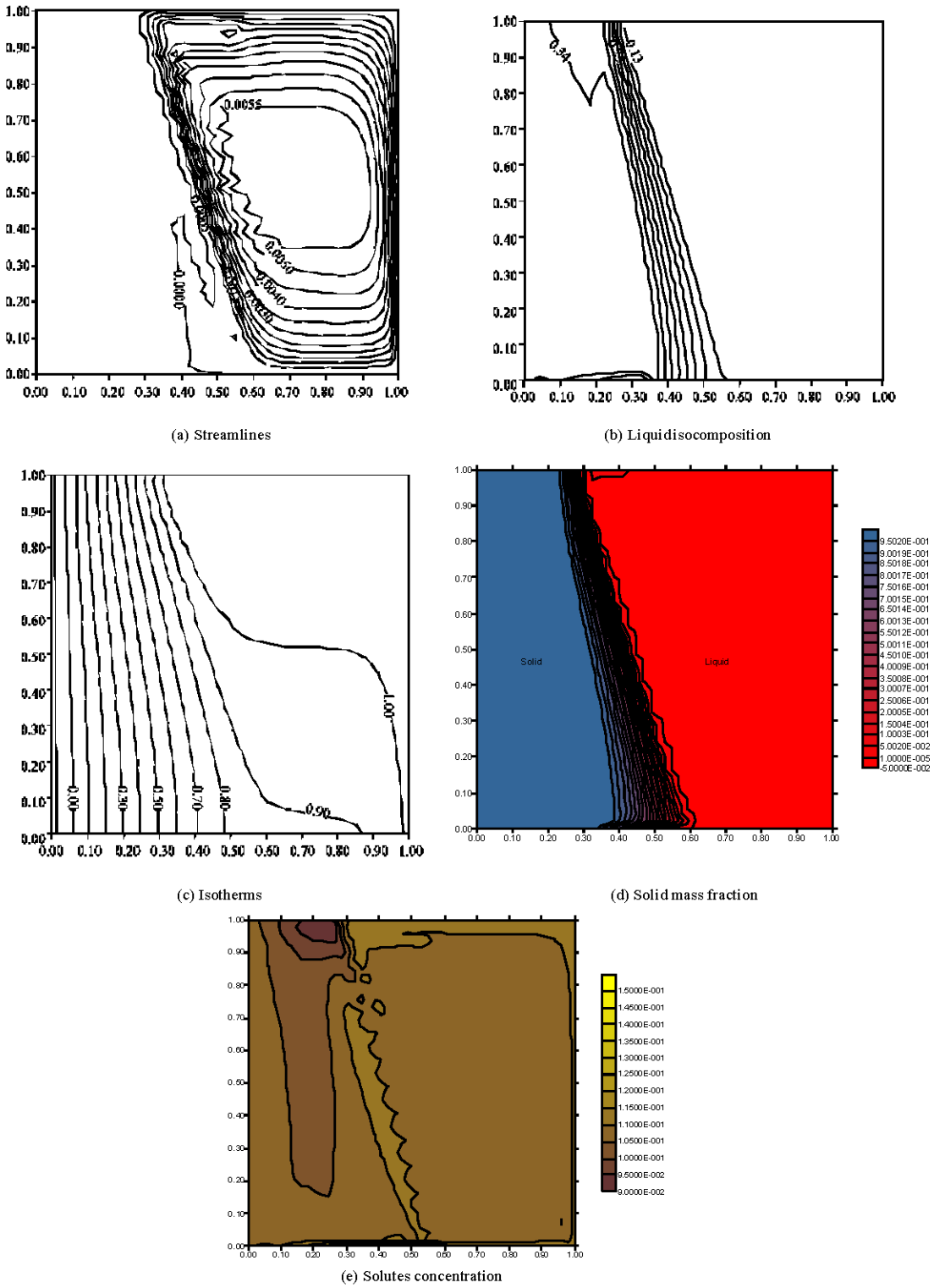

Fig. 4: Solidification at time = 500, (a) Streamlines, (b) Liquid isocomposition (c) Isotherms, (d) Solid mass fraction and (e) Solutes concentration

Convection flow field: Figure 3a shows the reversal flow, provoked by coupled effects of electromagnetic and buoyancy driven convection, observed in the melt, after the thermally dominated initial transient has passed, at which time the fluid has essentially lost some superheat. For this stage of solidification the mushy is expanding which increases the solutes rejected i.e., solute concentration gradient. While, the temperature gradient is weakening, due to shrinking of melted region. But the thermal buoyancy force driven convection remain the dominating force in the melt (since N = 0.59).

The rejected solutes will transported by the thermally convection flow in the melt for to be re-melting, as shown in Fig. 3e. The Lorentz force driven forced convection acts in opposition to thermal buoyancy force. Therefore, the externally magnetic field damped out turbulence and intensity of melt flow.

From this, it is result that the flow reversal observed in the melt region is weakening in strength and present a typical feature of natural convection coupled with forced convection in a stratified fluid.

Solute concentration and temperature fields: Isotherms, in Fig. 3c, show that the temperature is weakening in the melt region, which indicating that the fluid has lost some superheat.

In Fig. 3b, one can see that the mushy zone is expanding and becoming not uniform.

Figure 3b and e show the compositionally heavy fluid i.e., Carbon-rich fluid settles at the bottom and slowly forms a stratified layer. This layer continues to grow until the entire fluid composition evolves toward the eutectic at all levels. This process termed as laminar box-filling, (Sampath, 2001b). While the compositionally lighter fluid, i.e., Iron-rich fluid settles at the top. In addition, in Fig. 3e, one can see a multiple levels where the solutes are rejected in the mushy, especially near the bottom, which provoked instabilities in interface growth and influenced convective melt flow. The interface morphology is instable and of a form extremely complex, Fig. 3b. This is due to the interdentritic liquid flow in the mushy zone.

Solid mass fraction: Figure 3d shows the solid fraction formed for this stage of solidification. The composition of the solid product shown reflects the evolution of the fluid flow and solute concentration fields. In Fig. 3e, one can note the complex vertical variation in the solute concentration due to the melt flow.

Later stage of solidification: For the convective flow field, under an external magnetic field, streamlines, liquid isocompositions, isotherms, solid mass fractions and solutes distribution field corresponding to the stage of the solidification process, at t = 500, are presented in Fig. 4a-e, respectively.

Convection flow field: As the mushy zone continues to grow, the influence of solutal buoyancy gradually increases but it is remaining weak, since N = 0.59.

Here also the thermal buoyancy force driven convection is weakening, due to shrinking of melted region and decreasing of temperature gradient, see isotherms Fig. 4c.

For this stage of solidification the solutes rejected are increased. These solutes will be driven by thermal convection flow in the melt for to be re-melting and will be reintroduced in the mushy, as shown in Fig. 4e. Here also the Lorentz force driven forced convection flow acts in opposition to thermal convection flow, which induces that the externally magnetic field damped out turbulence and intensity of melt flow.

Also, here the flow reversal observed in the melt is a typical feature of natural convection coupled with forced convection flow in a stratified fluid (Sampath, 2001).

Solute concentration and temperature fields: Isotherms, in Fig. 4c, show that the temperature is weakening in the melt region.

Figure 3b and e show the compositionally heavy fluid settles at the bottom and slowly forms a stratified layer. This layer continues to grow until the entire fluid composition evolves toward the eutectic at all levels. While, the compositionally lighter fluid settles at the top.

In Fig. 4e, one can see that the solutes rejected are more important for this stage of solidification, which provoked instabilities in interface growth and influenced convective melt flow. Also, the interface morphology is more instable and of a form extremely complex, as shown in Fig. 4b.

Solid mass fraction: Also, the composition of the solid product shown in Fig. 4d reflects the evolution of the fluid flow and solute concentration fields. Here also we can note the complex vertical variation in the solute composition due to the melt flow, Fig. 4e.

CONCLUSION

In the present study problem on coupled effects of electromagnetic forced convection flow and buoyancy driven convection flow, in the molten Fe-0.42wt%C filled in a rectangular mold has been investigated numerically by employing the finite volume method. Results, obtained, have been shown the positive effect of the external

magnetic field in flow control which therefore reduced defects such as macrosegregation, microsegregation etc.

It is being realized that there is tremendous potential in using magnetic fields to control growth conditions in binary alloy systems. Magnetic field enhances micro-structural properties through melt flow control, thereby improving the homogeneity of the solid formed.

Finally, it requires to be mentioned that solutions of the present problem could be investigated for other Iron-Carbon systems, especially Fe-1wt%C and for case where the magnetic field is variable and the cases where it is applied in other directions.

REFERENCES

Anwar Hossain, M., M.Z. Hafizb and D.A.S. Rees, 2005. Buoyancy and thermocapillary driven convection flow of an electrically conducting fluid in an enclosure with heat generation. Int. J. Thermal. Sci., 44: 676-684.

Beckermann, C., 2002. Modelling of macrosegregation: Applications and future needs. Int. Mater. Rev., 47: 243-261.

Bennon, W.D. and F.P. Incropera, 1987. A continuum model for momentum, heat and species transport in binary solid-liquid phase change systems: I- Model formulation. Int. J. Heat Mass Transfer, 30: 2161-2170.

Liu, W., 2004. Finite element modelling of macrosegregation and thermomechanical phenomena in solidification processes. Ph.D Thesis, Ecole des Mines de Paris, France.

Ma, C.W., H.F. Shen, T.Y. Huang and B.C. Liu, 2004. Numerical simulation of macro-segregation in steel ingot during solidification. J. Acta Metallurgica Sin., 17: 288-294.

Mechighel, F. and M. Kadja, 2006. Thermo-solutal convection modelling during directional solidification of a binary conducting alloy in the presence and without a magnetic field. In: Proceedings of the 15th International Conference on Applied Simulation and Modelling, 26-28 June 2006, Rhodes, Greece. IASTED Organization.

Mittal, V., M.F. Baig and B. Kant Khan, 2005. Buoyancy-driven convection in liquid metals subjected to transverse magnetic fields. J. Ind. Institute Sci., 85: 119-129.

Patankar, S.V., 1980. Numerical Heat Transfer and Fluid Flow. McGraw-Hill, New York.

Sampath, R. and N. Zabaras, 2001. Adjoint variable method for the thermal design of eutectic directional solidification processes in an open-boat configuration. Numerical Heat Transfer, 39 Part A: 655-683.

Sampath, R., 2001. The adjoint method for the design of directional binary alloy solidification processes in the presence of a strong magnetic field. Ph.D Thesis, Cornell University, Ithaca, New York, USA.

Schneider, M.C. and C. Beckermann, 1995a. Formation of Macrosegregation by Multicomponent Thermosolutal Convection during Solidification of Steel Metall. Mater. Trans., 26 Part A: 2373-2388.

Schneider, M.C. and C. Beckermann, 1995b. Simulation of Micro-Macrosegregation during Solidification of a Low-alloy Steel. ISIJ Int., 35: 665-672.

Singh, A.K. and B. Basu, 2001. Modelling of convection during solidification of metal and alloys. Sadhana, 26: 139-162.

Singh, A.K. and B. Basu, 2001. Numerical study of effect of cooling rate on double-diffusive convection and macrosegregation in iron-carbon system. ISIJ Int., 41: 1481-1487.